

## RESEARCH ARTICLE

# Small molecule inhibition of lysine-specific demethylase 1 (LSD1) and histone deacetylase (HDAC) alone and in combination in Ewing sarcoma cell lines

Darcy Welch<sup>1,2</sup>, Elliot Kahen<sup>1,2</sup>, Brooke Fridley<sup>3</sup>, Andrew S. Brohl<sup>4,5</sup>, Christopher L. Cubitt<sup>2</sup>, Damon R. Reed<sup>1,4,5,6\*</sup>

**1** Sunshine Lab, H. Lee Moffitt Cancer Center and Research Institute, Tampa, Florida, United States of America, **2** Translational Research Core, H. Lee Moffitt Cancer Center and Research Institute, Tampa, Florida, United States of America, **3** Department of Biostatistics, H. Lee Moffitt Cancer Center and Research Institute, Tampa, Florida, United States of America, **4** Sarcoma Department, H. Lee Moffitt Cancer Center and Research Institute, Tampa, Florida, United States of America, **5** Chemical Biology and Molecular Medicine Program, H. Lee Moffitt Cancer Center and Research Institute, Tampa, Florida, United States of America, **6** Adolescent and Young Adult Program, H. Lee Moffitt Cancer Center and Research Institute, Tampa, Florida, United States of America

☞ These authors contributed equally to this work.

‡ These authors also contributed equally to this work.

\* [damon.reed@moffitt.org](mailto:damon.reed@moffitt.org)



## OPEN ACCESS

**Citation:** Welch D, Kahen E, Fridley B, Brohl AS, Cubitt CL, Reed DR (2019) Small molecule inhibition of lysine-specific demethylase 1 (LSD1) and histone deacetylase (HDAC) alone and in combination in Ewing sarcoma cell lines. PLoS ONE 14(9): e0222228. <https://doi.org/10.1371/journal.pone.0222228>

**Editor:** Arun Rishi, Wayne State University, UNITED STATES

**Received:** June 26, 2019

**Accepted:** August 23, 2019

**Published:** September 24, 2019

**Peer Review History:** PLOS recognizes the benefits of transparency in the peer review process; therefore, we enable the publication of all of the content of peer review and author responses alongside final, published articles. The editorial history of this article is available here: <https://doi.org/10.1371/journal.pone.0222228>

**Copyright:** © 2019 Welch et al. This is an open access article distributed under the terms of the [Creative Commons Attribution License](https://creativecommons.org/licenses/by/4.0/), which permits unrestricted use, distribution, and reproduction in any medium, provided the original author and source are credited.

**Data Availability Statement:** All relevant data are within the manuscript and its Supporting Information files.

## Abstract

Ewing Sarcoma (ES) is characterized by recurrent translocations between *EWSR1* and members of the ETS family of transcription factors. The transcriptional activity of the fusion oncoprotein is dependent on interaction with the nucleosome remodeling and deacetylase (NuRD) co-repressor complex. While inhibitors of both histone deacetylase (HDAC) and lysine-specific demethylase-1 (LSD1) subunits of the NuRD complex demonstrate single agent activity in preclinical models, combination strategies have not been investigated. We selected 7 clinically utilized chemotherapy agents, or active metabolites thereof, for experimentation: doxorubicin, cyclophosphamide, vincristine, etoposide and irinotecan as well as the HDAC inhibitor romidepsin and the reversible LSD1 inhibitor SP2509. All agents were tested at clinically achievable concentrations in 4 ES cell lines. All possible 2 drug combinations were then tested for potential synergy. Order of addition of second-line conventional combination therapy agents was tested with the addition of SP2509. In two drug experiments, synergy was observed with several combinations, including when SP2509 was paired with topoisomerase inhibitors or romidepsin. Addition of SP2509 after treatment with second-line combination therapy agents enhanced treatment effect. Our findings suggest promising combination treatment strategies that utilize epigenetic agents in ES.

## Introduction

Ewing sarcoma (ES) is the second most common bone sarcoma affecting children and adolescents. Despite advancements in treatment leading to improved outcomes for localized disease

**Funding:** This study was generously supported by the National Pediatric Cancer Foundation ([www.nationalpcf.org](http://www.nationalpcf.org)). This work has been supported in part by the Translational Research Core at the H. Lee Moffitt Cancer Center & Research Institute, a NCI designated Comprehensive Cancer Center (P30-CA076292). The funders had no role in study design, data collection and analysis, decision to publish, or preparation of the manuscript.

**Competing interests:** The authors have declared that no competing interests exist.

**Abbreviations:** LSD1, lysine-specific demethylase 1; ES, Ewing sarcoma; NuRD, nucleosome remodeling and deacetylase co-repressor complex; HDAC, histone deacetylase; 4HC, 4-hydroxycyclophosphamide; FA, fraction affected; FAD, flavin adenine dinucleotide; CI, combination index; IC<sub>50</sub>, half maximal inhibitory concentrations; C<sub>max</sub>, maximal plasma concentrations; AUC, area under the curve; MTIC, (5E)-5-(methylamino)hydrazinylideneimidazole-4-carboxamide.

over time, prognoses remain poor for patients with recurrent or metastatic disease [1]. ES is characterized by translocations involving members of the *ETS* family of transcription factors, most commonly t(11;22)(q24;q12) between the amino terminus of the *EWSR1* gene and the carboxy terminus of the *FLI1* gene, occurring in 85–90% of cases [2, 3]. Efforts to directly target the translocation were reenergized by publication of the ES genomic landscape by three groups demonstrating this alteration to be the only sufficiently recurring change across tumor samples [4–6].

The fusion oncoprotein EWS-FLI1 is considered a transcriptional activator in ES which is required for its oncogenic activity [3]. A proposed method of targeting the function of the fusion protein is by inhibiting other proteins that may assemble into functional complexes with EWS-FLI1 [7]. EWS-FLI1 transcriptional repression is mediated through direct binding with the nucleosome remodeling and deacetylase (NuRD) complex. The NuRD complex consists of histone deacetylases (HDACs), lysine-specific demethylase-1 (LSD1), and other DNA binding proteins and has been shown to play a role in tumor development as well as the general repression of transcription [3, 8]. Disrupting the NuRD complex through inhibition of LSD1, HDAC1, or HDAC2 may block EWS-FLI1 from affecting the transcription of oncogenic targets. Recent studies have demonstrated that direct targeting of LSD1 with molecular tools leads to significant attenuation of cancer cell proliferation in multiple models [9–11]. Importantly, in preclinical models of ES, reversible inhibitors of LSD1 also demonstrate some promise in halting tumor cell propagation [12]. This strongly influenced our decision to select SP2509 (previously HCI2509) for our studies in lieu of irreversible LSD1 inhibitors such as GSK2879552 or ORY-1001 which have been shown to interfere with flavin adenine dinucleotide (FAD) binding which LSD1 utilizes in histone lysine methylation [13], thereby failing to reduce cell viability in the models tested [14–16]. Additionally, these catalytic inhibitors of LSD1 have been previously tested in ES and found to be insufficient as a therapeutic strategy [17, 18]. SP2509 does not interfere with FAD binding as it interacts with the H3 pocket region of LSD1 which functions as an allosteric site, suggesting that SP2509 may act as an allosteric inhibitor [14]. SP2509 is also currently in Phase I clinical testing (NCT03600649).

HDAC inhibitors have been shown to possess direct antineoplastic activity as well as to enhance the efficacy of other anticancer agents [19]. There is also evidence that inhibition of HDAC inhibition attenuates LSD1 activity *in vivo* [20]. Despite lackluster results of HDAC therapy in sarcomas, we felt this class warranted investigation as a comparator to LSD1 inhibition due to both being present in the NuRD complex [21, 22].

Due to the rarity of Ewing sarcoma, clinical trials are difficult and time consuming to conduct, increasing the need for preclinical data to direct clinical trials. By targeting the NuRD complex along with agents known to provide clinical benefit we hoped to gain insight into whether or not particular combinations of agents were synergistic or antagonistic. We previously developed a system to efficiently evaluate combinations of interest across multiple cell line models with the goal of rapid translation into relevant clinical trials [23, 24]. Our methodology has been optimized to incorporate past lessons learned from *in vitro* experiments that did not translate well in clinical applications due to unachievable lengths of exposure or metabolic restraints [25, 26]. All experimental considerations for combination therapy were developed and conducted with the end thought being the eventual clinical trial. We sought to assess LSD1 inhibition and HDAC inhibition in combination with active chemotherapies currently utilized in ES care.

## Materials and methods

### Investigational agents

Agents used included current standard of care for ES and those of experimental interest (Table 1). Due to the instability of 4-hydroperoxy cyclophosphamide (4HC) and the reversible

**Table 1. Summary of agents tested, mechanism of action, selected pharmacokinetic data, and experimental values—top concentrations and AUC at top concentrations for each drug in each cell line.**

Agent	Mechanism of Action / Reference	Cmax (ng/ml)	AUC (h <sup>3</sup> ng/ml)	Cell Line Top Conc (ng/ml); AUC at Top Conc (ng/ml <sup>3</sup> 24hr)			
				A673	RD-ES	TC32	TC-71
4HC <sup>1</sup>	DNA Crosslinking, DNA Damage	6927	27700–33000	2000; 48000	2000; 48000	4000; 96000	4000; 96000
	<i>McCune JS, et al.(2009) J Clin Pharm; Kahen EJ, et al.(2016) Can Chem Pharm</i>						
Doxorubicin	DNA, topo II	2109	945	160; 3840	600; 14400	80; 1920	160; 3840
	<i>Greene RF, et al.(1983) Cancer Res; Bartlett NL, et al.(1994) J Clin Oncol</i>						
Etoposide	Topoisomerase II, DNA Damage	20000	157000	300; 7200	800; 19200	800; 19200	800; 19200
	<i>Kaul S, et al. (1995) Anticancer Drugs</i>						
Romidepsin	Class I/II HDAC	377	2414	4; 96	4; 96	4; 96	4; 96
	<i>Fouladi M, et al.(2006) J Clin Oncol</i>						
SN-38 <sup>2</sup>	Topoisomerase IB	30	104	1; 24	0.75; 18	0.75; 18	0.75; 18
	<i>Ma MK, et al.(2000) Clin Cancer Res</i>						
SP2509 <sup>†</sup>	LSD1 inhibitor	3000	TBD	1000; 72000	1000; 72000	2000; 144000	2500; 180000
	<i>Fiskus W., et al.(2012) J Clin Oncol</i>						
MTIC <sup>3</sup>	Alkylator	13000	46000	250; 6000	NA	250; 6000	NA
	<i>Horton TM, et al.(2007) J Clin Oncol</i>						
Vincristine	Microtubules, Anti-mitotic	40	90	2; 48	0.6; 14.4	2; 48	3; 72
	<i>Guilhaumou R, et al.(2011) Cancer Chemother Pharmacol</i>						

†Value determined in rats

<sup>1</sup>Active metabolite of cyclophosphamide

<sup>2</sup>Active metabolite of irinotecan

<sup>3</sup>Active metabolite of temozolomide

<https://doi.org/10.1371/journal.pone.0222228.t001>

LSD1 inhibitor SP2509, fresh drug solutions were prepared in DMSO prior to every experiment. MTIC ((5E)-5-(methylaminohydrazinylidene)imidazole-4-carboxamide, the active metabolite of temozolomide) was prepared in 100% ethanol and then mixed 1:1 with media immediately prior to application. Final ethanol concentration never exceeded 1%. Stock solutions for all other compounds were made in DMSO and stored at -20°C. All agents were obtained directly from Selleck Chemicals (Houston, TX, USA), and Sigma-Aldrich (St. Louis, MO, USA). Structures for all agents are available in public databases.

### Cell culture

We selected four ES cell lines that are well characterized and commonly used in recent studies (Table 2) [3, 12, 27]. A673 was obtained from the ATCC (Manassas, VA). The TC32 (Children’s Oncology Group (COG) Cell Line & Xenograft Repository), TC-71 (National Cancer Institute (NCI) Pediatric Preclinical Testing Program) and RD-ES cells lines were generously shared by Dr. Stephen Lessnick. A673 Cells were maintained in DMEM with 10% fetal bovine serum. TC-71, RD-ES and TC32 cells were maintained in RPMI with 15% fetal bovine serum. While protein binding can impact the activity of anti-cancer agents [28], these 15% concentrations are higher than human albumin concentrations. Media was supplemented with PenStrep prior to extended incubation times. Cells were grown at 37°C and 5% CO<sub>2</sub>. All cell lines tested

Table 2. Summary of Ewing cell lines.

Cell Line	ATCC Designation	Tissue	Doubling Time (hours)	Diagnosis	Patient Info	EWS-FLI1 translocation t (11;22)(q24;q12)	FLI1-EWS Reciprocal Fusion	TP53	KDM1A mRNA Expression Level <sup>g</sup>	STAG2 Status <sup>h,i</sup>
A673	ATCC <sup>®</sup> CRL-1598 <sup>™</sup>	Muscle <sup>a</sup>	25 <sup>c</sup>	Ewing's Sarcoma <sup>a</sup>	15 year old female <sup>a</sup>	Type 1 Fusion <sup>d</sup>	Detectable <sup>d</sup>	Non-functional (p.A119 frameshift) <sup>c,f</sup>	8.49 ± 1.29	Wildtype
RD-ES	ATCC <sup>®</sup> HTB-166 <sup>™</sup>	Bone <sup>a</sup>	60 <sup>k</sup>	Ewing's Sarcoma <sup>a</sup>	19 year old male <sup>a</sup>	Type 2 Fusion <sup>e</sup>	Unknown	Mutant (p. R273C) <sup>f</sup>	5.66 ± 0.75	No Expression
TC32	N/A	Bone <sup>b</sup>	24 <sup>c</sup>	PNET <sup>b</sup>	17 year old female <sup>b</sup>	Type 1 Fusion <sup>c</sup>	Unknown	Functional (Wildtype) <sup>c</sup>	2.32 ± 0.23	I636sf
TC-71	N/A	Ileum <sup>c</sup>	21 <sup>c</sup>	Ewing's Sarcoma <sup>b</sup>	22 year old male <sup>b</sup>	Type 1 Fusion <sup>d,e</sup>	Undetectable <sup>d</sup>	Non-functional (p.R213 nonsense) <sup>c,f</sup>	3.14 ± 0.50	Wildtype

<sup>a</sup>ATCC

<sup>b</sup>Children's Oncology Group (COG) Cell Culture and Xenograft Repository

<sup>c</sup>May, W.A., et al. Characterization and Drug Resistance Patterns of Ewing's Sarcoma Family Tumor Cell Lines. *PLoS One*. 2013; 8(12): e80060.

<sup>d</sup>Elzi, D.J., et al. The role of FLI-1-EWS, a fusion gene reciprocal to EWS-FLI-1, in Ewing sarcoma. *Genes Cancer*. 2015 Nov; 6(11–12): 452–461.

<sup>e</sup>Huang, H.J., et al. R1507, an Anti-Insulin-Like Growth Factor-1 Receptor (IGF-1R) Antibody, and EWS/FLI-1 siRNA in Ewing's Sarcoma: Convergence at the IGF/IGFR/Akt Axis. *PLoS One*. 2011; 6(10): e26060.

<sup>f</sup>Tirode, F., Sirdez, D., et al. Genomic landscape of Ewing sarcoma defines an aggressive subtype with co-association of STAG2 and TP53 mutations. *Cancer Discov*. 2014 Nov; 4(11): 1342–1353.

<sup>g</sup>Pishas, P.I., et al. Therapeutic targeting of KDM1A/LSD1 in Ewing Sarcoma with SP-2509 Engages the Endoplasmic Reticulum Stress Response. *Molecular Cancer Therapeutics*. 2018 Sep; 17(9): 1902–1916.

<sup>h</sup>Crompton, B.D., et al [5]

<sup>i</sup>Brohl, A.S., et al [4]

<sup>k</sup>Hyper Cell Line Database

<https://doi.org/10.1371/journal.pone.0222228.t002>

free of mycoplasma using MycoAlert tests (Lonza Rockland, Rockland, ME). Cell line authentication was confirmed using StemElite ID system (Promega, Madison, WI) and comparing results to the ATCC, COG, and NCI short tandem repeats (STR) profiles.

### Cell viability assays

The activity of drugs alone and in combination was determined by a high-throughput cell viability assay as described previously [23, 24]. Cells (4.5 x 10<sup>3</sup> per well) were transferred to 384-well plates and incubated for 24 hours prior to drug administration, which was empirically confirmed to be a period of log-phase growth for these conditions. At 72 hours, cell viability was assessed using CellTiter-Glo (CT-Glo) (Promega, Madison, WI, USA), which provides luminescence proportional to cellular ATP levels. This reflects the reduction in cellular metabolism (an indication of cell viability) due to the drug treatment. Data were transferred to custom Microsoft Excel templates and the percent viability/fraction affected was calculated by normalization to untreated control conditions. Specifically, FA is calculated as FA = 1 - (CT-glo signal with drug treatment)/(CT-glo signal without drug treatment). Absolute IC50 values were determined using sigmoidal equilibrium model regression and fitted using XLfit version 5.5 (ID Business Solutions, Guildford, Surrey, England). The IC50 values obtained from single-drug viability assays were used to design subsequent drug combination experiments.

### Single-agent screening

Single agent dose response was characterized for a panel of 7 therapeutic candidates across 4 ES cell lines (A673, RD-ES, TC32 and TC-71) (Table 2). Human pharmacokinetic data was collected using pediatric and combination studies when available from previously reported Phase I trials. The majority of drugs selected (excluding only romidepsin and SP2509) have half-lives greater than 8 hours or have a continuous dosing schedule clinically. The half-life of SP2509 is unknown in humans. We chose to uniformly expose the cells for 72 hours to all the drugs. Experiments were performed in triplicate with at least 4 technical replicates per biological replicate.

### Two-drug combination screening

A 5x5 checker-board matrix was used to assess all two-drug combinations at five clinically achievable concentrations. Each combination was evaluated at multiple drug ratios to identify synergy. Analysis of additive and synergistic effects was done by measuring cell viability with the CellTiter-Glo assay with results analyzed using the Combination Index (CI) method of Chou-Talalay [29]. CI, a measure of drug synergy, is derived by taking the dose-effect curve for each drug using the median effect principle and then comparing it to the effect achieved with the 2-drug combination. 2-drug combination activity that is merely additive is represented by a CI value of 1.0. As CI decreases below 1.0, drug synergism increases. Antagonistic drug effects are indicated by a CI greater than 1.0. A minimum of two biological replicates per cell line were performed with at least 4 technical replicates per condition in each experiment.

### Order of addition assays

A673 and TC32 cells ( $2.25 \times 10^3$  and  $4.5 \times 10^3$  per well, respectively) were transferred to 384-well plates and incubated for 24 hours prior to initial drug administration. Cells were then treated with one, two or three drugs concurrently at the chosen top concentration, one half, and one quarter of the top concentration, and incubated for an additional 24 hours. Experimental plates were then read on Day 2 with RealTime-Glo (RT-Glo) (Promega, Madison, WI, USA) (proprietary technology) before being treated with an additional drug. Plates were then read a second time 72 hours later on Day 5, and final cell viability results were obtained. Experiments were performed in duplicate plus an additional run with higher cell numbers with 12 technical replicates per condition in each experiment.

### Statistical methods

The drug response data was modeled using a sigmoidal equilibrium regression curve using the software package XLfit version 5.5. Differences between drug response measurements (i.e., FA values) between drug combinations was completed using linear mixed effects model with a random intercept for cell lines to account for multiple measurements taken off the same cell line with a fixed effect adjustment for concentration level of the drug using R package *lme4*. For comparisons between the 21 drug combinations a Bonferroni adjustment for multiple testing was used.

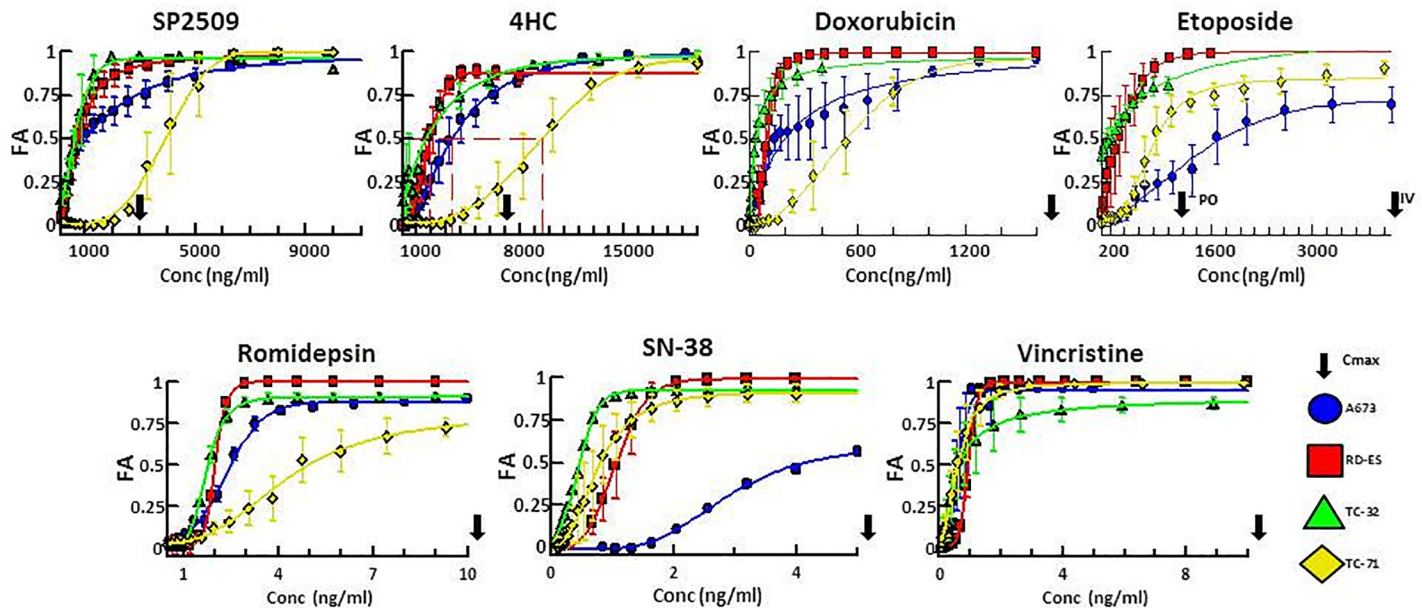


**Fig 1. Single agent dose response plots for 7 tested agents against 4 ES cell lines demonstrate efficacy at clinically achievable concentrations.** Dose response plots of each drug tested across 4 cell lines plotted as fraction affected (FA) versus concentration (ng/ml). Data was recovered 72 hours after drug treatment. Plotted points represent the mean FA values while error bars represent  $\pm$ SEM (standard error of the mean) between technical replicates. Arrows beyond the x-axis indicate a Cmax in excess of the values displayed.

<https://doi.org/10.1371/journal.pone.0222228.g001>

## Results

### NuRD complex directed therapeutics demonstrate considerable *in vitro* activity at clinically achievable levels

We characterized the single-agent activity of a panel of 7 therapeutic candidates (Table 1) using 4 ES cell lines (A673, RD-ES, TC32 and TC-71) (Table 2). The active metabolite of the alkylating prodrug cyclophosphamide, 4HC; the DNA intercalator and topoisomerase II inhibitor, doxorubicin; the topoisomerase II inhibitor, etoposide; the active metabolite of the topoisomerase I inhibitor irinotecan, SN-38; and the Beta-tubulin inhibitor, vincristine were chosen due to their role in first and second line treatment of ES. The additional 2 agents, the HDAC1 and HDAC2 inhibitor romidepsin and the reversible LSD1 inhibitor SP2509, were selected based on their respective targets in the NuRD complex [3]. To evaluate the potency of these agents, full dose-response curves were obtained for the drug panel in each cell line. As anticipated, cell lines showed sensitivity to agents used clinically in the management of ES. In addition, experimental candidates romidepsin and SP2509 demonstrated potency in the single agent context. The half maximal inhibitory concentrations (IC50s), simulated maximal plasma concentrations (Cmax), and area under the curves (AUC) were within clinically achievable levels for all drugs selected in nearly all contexts (Fig 1, Table 1, Table 2). Some variability between cell lines was observed with A673 and TC-71 demonstrating a trend towards tolerance relative to RD-ES and TC32; however, cell line drug sensitivities were mostly uniform across the cell lines and were uniform for vincristine. A673 demonstrated a relative tolerance to topoisomerase inhibitors while TC-71 was more tolerant to alkylators and epigenetic agents (S1 Table).

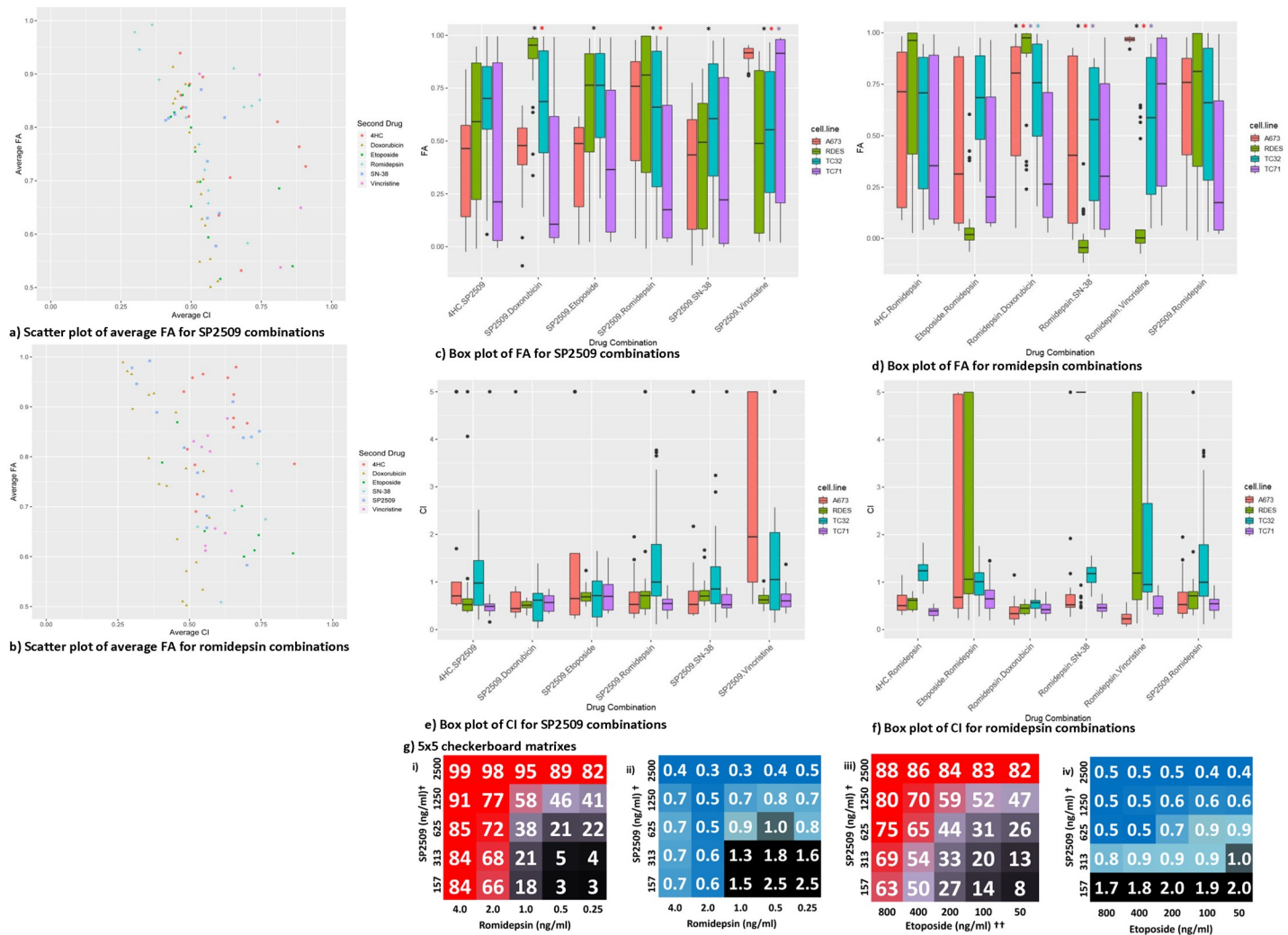


**Fig 2. Overview of combination efficacy for SP2509 and romidepsin combinations.** Scatter plots displaying the average fraction of cells affected (FA) for drugs paired with a) SP2509 and b) romidepsin. Box plot for c) SP2509 exhibiting the FA of each cell line for all drug combinations. A black asterisk indicates a significantly higher FA value than 4HC+SP2509. P-values as follows: SP2509+doxorubicin =  $1.87 \times 10^{-25}$ , SP2509+etoposide =  $2.54 \times 10^{-16}$ , SP2509+romidepsin =  $6.72 \times 10^{-15}$ , SP2509+SN-38 =  $2.81 \times 10^{-8}$ , SP2509+vincristine =  $1.02 \times 10^{-18}$ . A red asterisk indicates a significantly higher FA value than SP2509+etoposide. P-values as follows: SP2509+doxorubicin =  $1.66 \times 10^{-9}$ , SP2509+romidepsin =  $3.43 \times 10^{-6}$ , SP2509+vincristine =  $1.28 \times 10^{-11}$ . A purple asterisk indicates a significantly higher FA than SP2509+doxorubicin. P-value as follows: SP2509+Vincristine =  $3.19 \times 10^{-5}$ . Statistics based on combined value from all cell lines and all concentrations. Box plot for d) romidepsin exhibiting the FA of each cell line for all drug combinations. A black asterisk indicates significantly higher FA than romidepsin+etoposide. P-values as follows: romidepsin+doxorubicin =  $8.56 \times 10^{-7}$ , romidepsin+SN-38 =  $6.97 \times 10^{-7}$ , romidepsin+vincristine =  $7.23 \times 10^{-19}$ . A red asterisk indicates significantly higher FA than romidepsin+SP2509. P-value as follows: romidepsin+doxorubicin = 0.00011, romidepsin+vincristine =  $2.26 \times 10^{-12}$ . A purple asterisk indicates significantly higher FA value than romidepsin+4HC. P-value as follows: romidepsin+vincristine =  $8.11 \times 10^{-11}$ . Statistics based on combined value from all cell lines and all concentrations. Box plots for e) SP2509 and f) romidepsin exhibiting the CI for each cell line for all drug combinations. g) 5x5 Checkerboard matrixes assessing combination activity. i) FA and ii) CI values for SP2509 and romidepsin assessed at 25 different concentrations. †Alternate SP2509 concentrations used (1000, 500, 250, 125, 62.5ng/ml for A673 and RD-ES cell lines; 2000, 1000, 500, 250, 125ng/ml used for TC32 cell line). Variable concentrations used due to differences in IC<sub>50</sub> per cell line. iii) FA and iv) CI values for SP2509 and etoposide assessed at 25 different concentrations. ††Alternate etoposide concentrations used (300, 150, 75, 37.5, 18.8ng/ml used for A673 cell line).

<https://doi.org/10.1371/journal.pone.0222228.g002>

## The LSD1 inhibitor SP2509 and the HDAC inhibitor romidepsin are synergistic with conventional chemotherapeutic agents *in vitro*

We hypothesized that agents that interact with components of the NuRD complex would work synergistically with agents already utilized in the treatment of ES. We performed high throughput cell viability assays that assessed each of the 7 agents in combination at 25 different

concentration pairs. All drugs were tested below Cmax values and spanned the IC50 for each cell line to allow for synergy (combination index, CI) calculations. We identified multiple drug combinations that demonstrated high fraction affected (FA) values (see [methods](#) for further discussion of CI and FA). The FA and CI values of each drug combination and drug ratio in each individual cell line are summarized in [S2 Table](#) in order of top performing combinations. The average distribution of effects for each drug combination trends toward high FA and low CI values when paired with SP2509 or romidepsin. ([Fig 2A and 2B](#), respectively). SP2509 generally showed synergy with all drugs apart from vincristine which demonstrated antagonism at most concentrations in this combination. Combinations containing romidepsin, while still trending towards high FA and low CI, were less synergistic than those with SP2509 overall, experiencing antagonistic drug interactions with vincristine as well as etoposide. In order to gain a comprehensive overview of FA across all cell lines and concentrations, statistical analysis was performed using a linear mixed effects model with a random intercept for cell lines and a Bonferroni adjustment for multiple testing (adjusting for 210 tests, a p-value of 0.0002 is considered significant; see [methods](#) for further discussion of statistical analysis). Our analysis showed that of the six possible combinations with SP2509, all the combinations produced a more significant FA than SP2509+4HC ([Fig 2C](#)). Combinations SP2509+romidepsin, SP2509+doxorubicin, and SP2509+vincristine all produced FAs more statistically significant than SP2509+etoposide. And the FA of the SP2509+vincristine was more statistically significant than the combination of SP2509 with 4HC, etoposide, and doxorubicin. When the same analysis was performed with romidepsin combinations, we found romidepsin+doxorubicin, romidepsin+SN-38, and romidepsin+vincristine to have the most statistically significant FAs ([Fig 2D](#)). Romidepsin+vincristine had the most statistically significant FAs, more significant than when paired with etoposide, SP2509, and 4HC. Interestingly, nearly all the combinations produced higher FA values than those produced with romidepsin+SP2509.

When viewed comparatively between cell lines, sensitivity differences to combinations containing SP2509 or romidepsin were observed ([Fig 2C, 2D, 2E and 2F, S2 Table](#)). A673 was typically more resistant to drug pairs with SP2509 ([Fig 2C](#)). Except for SP2509+vincristine, FA values trended lower than the other cell lines, though this is likely due more to A673's sensitivity to vincristine. This sensitivity is likely to have skewed the statistical analysis for this combination, making the FA appear more significant for this combination than its actual performance across all the cell lines. RD-ES and TC32 were similar in their drug tolerances, mostly demonstrating high median and maximum FA values. TC-71 had the largest distributions of effects across all the combinations tested, though kill rates near 100% (FA near 1.0) were still reached for all combinations with SP2509. The distribution of CI values for SP2509 combinations was similar in RD-ES and TC-71 with median values between 0.5 and 0.8 ([Fig 2E](#)). SP2509 synergism in TC32 was more greatly distributed showing antagonism at some concentrations and synergism at others. FA values for combinations containing romidepsin were more mixed ([Fig 2D](#)). The most notable differences compared to SP2509 combinations include the relative resistance of RD-ES and the notable potency of romidepsin+vincristine in A673. Synergism was consistently observed in combinations containing romidepsin with TC32 displaying higher values at more concentrations than in other lines ([Fig 2F](#)). The resistance of RD-ES to these combinations is associated with highly distributed CI values. The combination of SP2509 with romidepsin itself was rather effective, producing median FA values near and above 0.7 across all cell lines except TC-71, with maximum FA values of 1.0 reached in all 4 ES models ([Fig 2A, 2B, 2C, 2D, 2G and 2I](#)). Synergy between the drugs was also consistently seen (average CI = 0.4), with TC32 having a bit of a larger distribution across all concentrations tested compared to the other lines ([Fig 2B, 2E, 2F and 2Gi](#)). Notably, even at lower concentrations of both drugs, high FA and low CI values were typically still observed.



Topoisomerase inhibitors showed particularly strong activity and synergy when paired with SP2509. SP2509 and any of doxorubicin, etoposide or SN-38 demonstrated an average FA of at least 0.87, with FA as high as 0.95 observed in two cell lines and average CIs of 0.5 or lower (Fig 2A, 2C, 2E and 2Giii,iv, S2 Table). We were particularly interested in the translational potential of combining SP2509 with etoposide since oral etoposide is often used in the relapsed setting, continuously dosed, and well tolerated in patients. At lower concentrations of etoposide, combined with the top concentration of SP2509, FA was 0.88 (Fig 2Giii) and minimum CI values of 0.4 (Fig 2Giv) were obtained. Synergy was achieved at all except the lowest concentrations of SP2509.

### SP2509 enhances efficacy of VIT (vincristine, irinotecan, and temozolomide)

In order to further investigate the translational potential of SP2509, we administered it in combination with the conventional treatment utilized in relapsed ES, VIT: Vincristine, Irinotecan (SN-38, the active metabolite), and temozolomide (MTIC, the active metabolite)[30, 31]. We chose two cell lines, A673 and TC32, which we felt would be representative of our cell lines and had diversity amongst the other genes that may play a role in eventual subtyping of Ewing sarcoma, *TP53* and *STAG2*. TC32 has a functional p53 gene while A673 has a frameshift mutation rendering p53 nonfunctional. Conversely, A673 is wild type for *STAG2* whereas TC32 has a frameshift mutation in *STAG2* (Table 1) [4, 27, 32]. We assayed for potential differences in potency with this 4-drug combination by testing multiple orders of addition of the agents as well as one half and one quarter concentrations of what we estimated would be an optimal top concentration (Fig 3A and 3B, S1 Fig). Utilizing RT-Glo, we were able to obtain multiple time-points of the same experimental plate, which allowed us to observe drug kinetics over time. We found that the effects on viability from SN-38 were more delayed than any of the other agents. This was most noticeable in A673 where there was a 50-fold shift in the IC<sub>50</sub> between 24-hours and 96-hours (40ng/ml vs 0.77ng/ml, respectively) (Table 3). The practical result of this is that combination FAs were typically higher when SN-38 was added first rather than second (Fig 3A and 3B; S1 Fig). TC32 appears to be more sensitive overall with the exception of vincristine, though this may simply be due to the differences in doubling times. Indeed, because of the speed of A673 proliferation, cell numbers needed to be halved to make it compatible with this protocol due to considerable variability between experiments (S1C Fig). The particular sensitivity of A673 to vincristine in this context is worth further study. Importantly, at concentrations well below C<sub>max</sub> (Table 3, S1A Fig), combinations of VIT+SP2509 were able to reduce cell viability by over 90% at the highest-tested concentrations and by over 80% at half the topmost concentrations. It should be noted that due to the instability of MTIC, the actual concentrations in media are likely below the calculated estimate. In A673, there is no clear preference for any particular order of addition with these 4 agents, though the largest increase between Day 2 and Day 5 was seen when SP2509 was added last. In TC32, there is a tendency towards higher potency when SP2509 is added last, but this is within the bounds of experimental variability. Overall, addition of SP2509 increased the FA but only slightly, most likely due to the already efficacious treatment of VIT alone. However, this increase can be noted at lower concentrations as well as when SP2509 is substituted for one of the other drugs in combination (S1 Fig).

## Discussion

In this study, our aim was to evaluate the inclusion of romidepsin and SP2509, both NuRD complex-directed therapeutics, with agents currently utilized in the treatment of ES. Our results confirm that ES cell lines are sensitive to multiple chemotherapeutic agents commonly

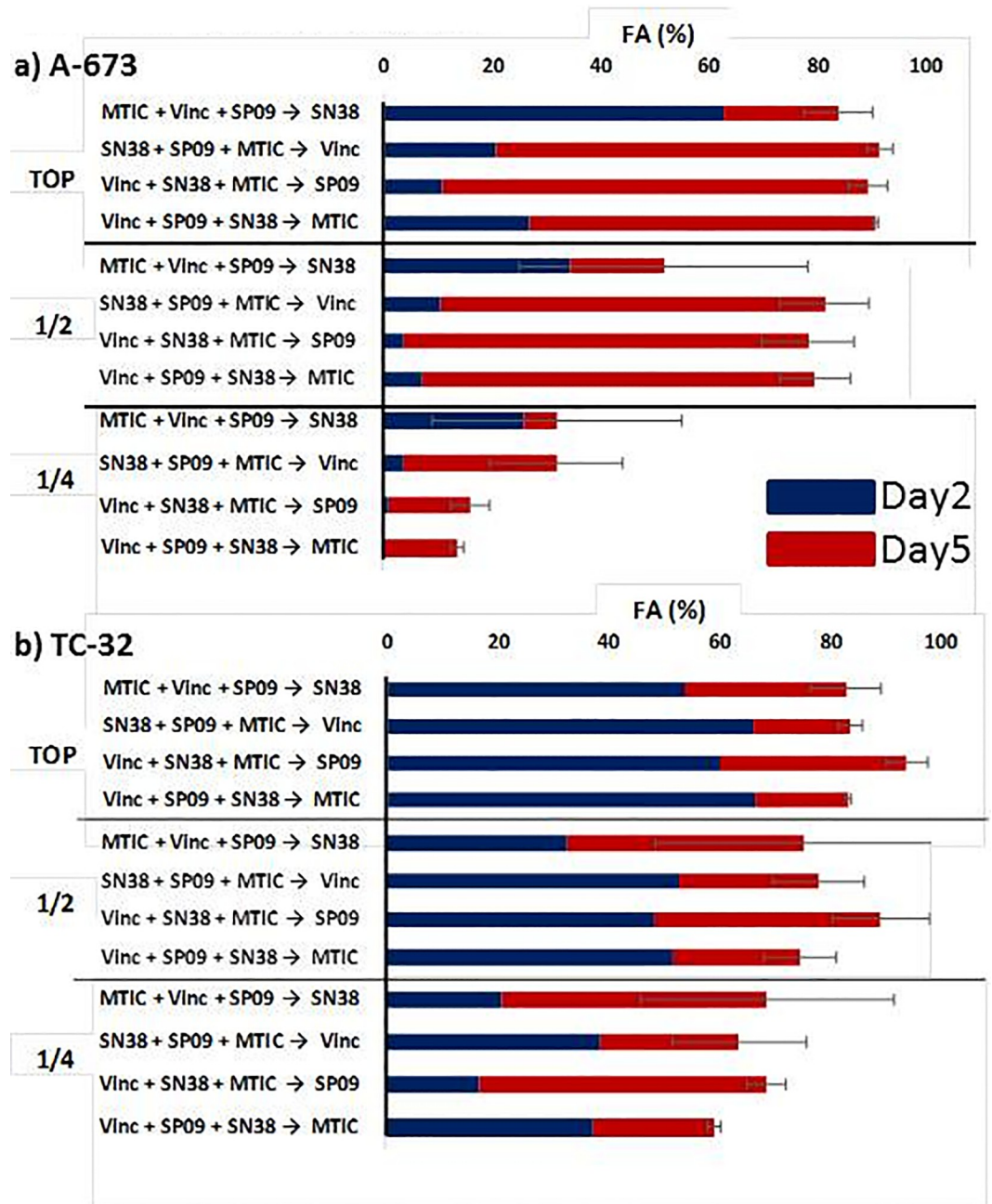


**Fig 3. Vincristine, irinotecan, temozolomide, and SP2509 order of addition.** Results of order of addition experiments for a) A673 and b) TC32, respectively. One to three drugs were given concurrently 24 hours after plating and read on Day 2. The fourth drug was added after the 48 hour read and the same experimental plate was read on Day 5. TOP represents the highest concentration used as indicated in Table 3B; 1/2 is half the highest concentration, 1/4 is a quarter of the highest concentration. Error bars represent standard error of the mean. A673 n = 2, TC32 n = 4. See S1 Fig for all order of addition results.

<https://doi.org/10.1371/journal.pone.0222228.g003>

used in ES treatment and the addition of NuRD complex-directed drugs show promising results as potential additions to future chemotherapeutic regimens. A summary of the top performing agents is included in S3 Table. When considering promising agents for ES, the practicalities of the chemotherapeutic regimen should be considered early in order to best inform eventual trial approaches which will incorporate a new agent. Standard initial therapy for ES

Table 3. Single agent dose response IC<sub>50</sub>s at 24-hours and 96-hours after treatment, ± standard error of the mean.

Tx	A673		TC32		Top Concentration	Cmax (ng/ml)
	Day 2	Day 5	Day 2	Day 5		
MTIC	18889 ± 3240	18915 ± 3672	15547 ± 7867	9447 ± 4045	250	276
SN38	40 ± 33	0.77 ± 0	4.0 ± 0.5	2.6 ± 0.2	4	30
SP2509	4222 ± 863	1171 ± 212	2375 ± 221	1238 ± 89	1000	3000
Vincristine	0.73 ± 0.25	0.79 ± 0.03	6.2 ± 1.4	2.0 ± 0.3	1	40

<https://doi.org/10.1371/journal.pone.0222228.t003>

includes a clinical trial when available and in the United States typically is based on every 2 week therapy with vincristine, doxorubicin and cyclophosphamide alternating with ifosfamide and etoposide [33]. Relapse studies typically incorporate a camptothecin (either topotecan or irinotecan) with an alkylating agent (typically cyclophosphamide or temozolomide respectively) or oral etoposide when a trial is not available [34].

As of this writing, optimal schedule, toxicities, adverse effects and maximal tolerated doses with resultant PK are not yet available for reversible LSD1 inhibitors in humans. Trials are open with SP2577, a similar compound, in the Ewing sarcoma population with continuous dosing schedules, NCT03600649. Importantly, when SP2509 is combined with current second-line conventional chemotherapy regimen vincristine, irinotecan, temozolomide (VIT) *in vitro*, cell viability is considerably decreased even at concentrations well below Cmax. The concentrations used in these experiments are well below the observed maximal plasma concentrations observed in pharmacokinetic assays and thus it is possible that sufficient efficacy could be achieved at lower than maximally tolerated doses, which may minimize side effects and maximize additional agents being combined in the future. 4HC, etoposide, doxorubicin, and SN-38 all exhibited robust activity alone and in combination with SP2509, which was confirmed when we performed a correlation analysis on the FA of all combinations tested (Fig 4). If indeed SP2509 is acting as an LSD1 inhibitor, LSD1 is required for heterochromatin formation [35, 36]. When inhibited, DNA would be structurally less dense and more open to agents that damage DNA such as topoisomerases, which correlates well with our findings.

Of note is the antagonism exhibited when SP2509 and vincristine are paired in the A673 cell line. A possible explanation is the unique sensitivity of A673 to vincristine, disallowing synergy. Inhibition of the EWS-FLI1 fusion protein has been shown to decrease EWS-FLI1-mediated generation of microtubule-associated proteins leaving cells more susceptible to microtubule depolymerization by vincristine [37]. Real time quantitative PCR for the EWS/ETS gene product as well as the native FLI1 showed the lowest expression of EWS/ETS in A673, followed by TC32 and then TC-71 (RD-ES was not tested) [38]. However, it has also been shown that levels of the EWS-FLI1 transcript and protein are heterogeneous from one cell to another and can range from low to high expression levels and fluctuate along time, producing different phenotypes of cell proliferation, migration, invasion and metastases [39]. Clearly more investigation is required before a definitive assessment of these mechanisms can be ascertained. Another possibility is that the cell lines have relative resistance to vincristine from prior exposure. Indeed, TC-71 and TC32 were derived post chemo, RD-ES was derived from a primary osseous of the humerus, and it is unknown whether A673 was derived pre- or post-chemotherapy. A673 was derived in 1973 and it is known that lower doses of chemotherapy were administered then, but vincristine most likely would have been used [38]. This does not seem to be generalizable to all microtubule inhibitors as when SP2509 was administered with docetaxel to prostate cells, synergy is noted at sub-IC<sub>50</sub> doses [40].

Another possible translational route would be combining an epigenetic agent with oral etoposide. This route has the advantages of long exposures of both agents at effective

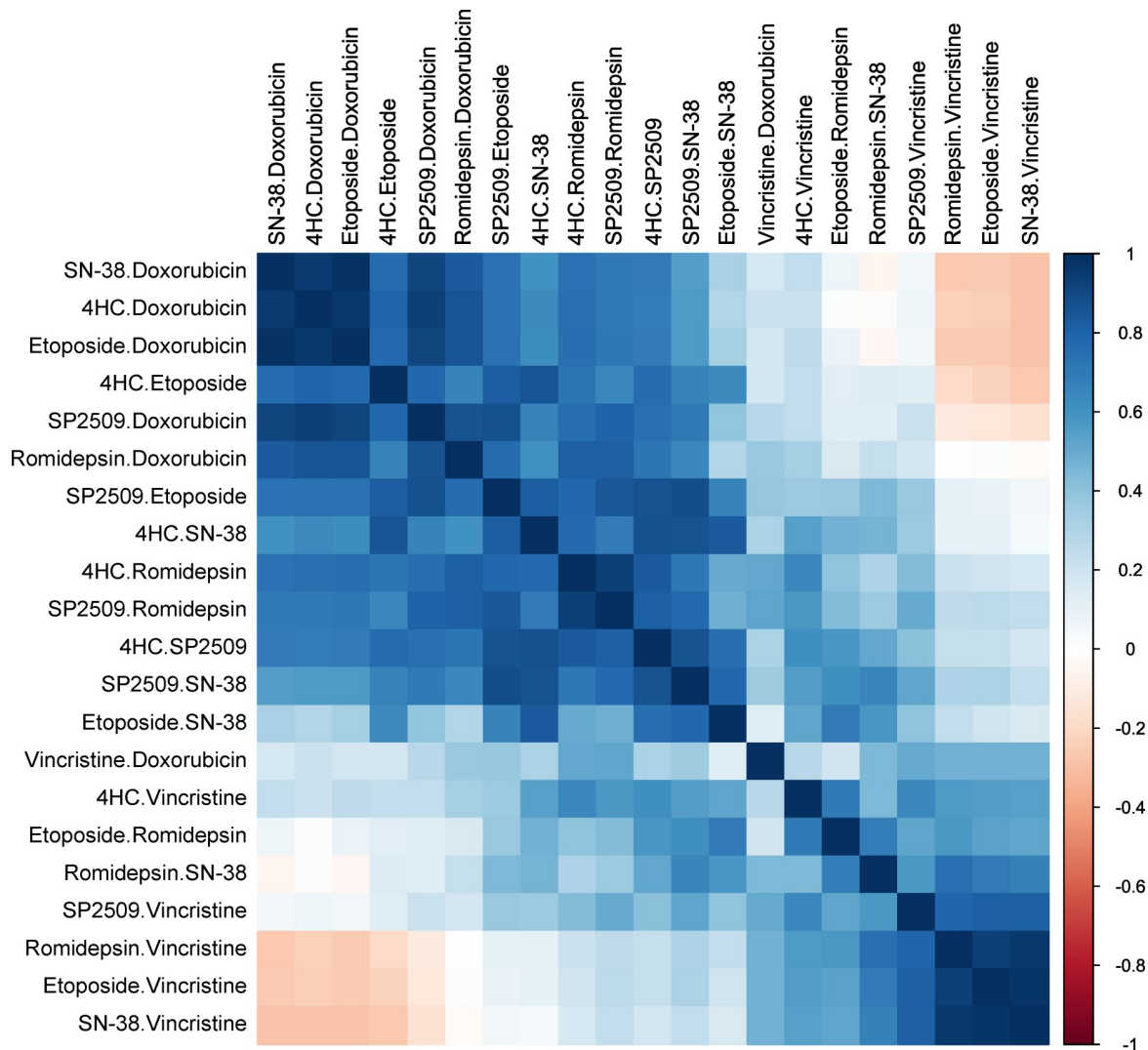


**Fig 4. Correlation analysis of FA for all combinations tested.** Spearman correlation between FA values from four cell lines treated with the various drug combinations. Blue values indicate strong positive correlation while red values indicate strong negative correlation between drug FA values.

<https://doi.org/10.1371/journal.pone.0222228.g004>

concentrations along with the fewest side effects of the chemotherapeutic backbone. An additional potential advantage of combination strategies utilizing SP2509 beyond its distinct mechanism of action is the potential feasibility of continuous dosing. We postulated a clinical dosing schedule for one week with oral etoposide paired with SP2509 and romidepsin (Fig 5). In the case of SP2509 and etoposide, multiple opportunities for synergism exist at the concentrations used and times administered. Recent combination data with vincristine and translocation targeting agents such as TK216 are also being reported [37]. The findings here of synergy and activity at low levels are especially interesting due to their clinical applications.

We demonstrated that the HDAC inhibitor romidepsin would also be a promising addition to standard chemotherapy agents utilized in relapsed or refractory Ewing sarcoma. Even though multiple opportunities for synergism do not exist as in the case of etoposide and SP2509, romidepsin has been shown here to be effective even at lower concentrations and could prove synergistic beyond the levels we tested. Epigenetic modification is particularly of

	ng/ml	D1		D2		D3		D4		D5		D6		D7		
SP2509 PO <sup>2</sup>	2442															
Rat PK only available	1221	70		70		70		70		70		70		70		
Theoretical	610.5	44		44		44		44		44		44		44		
Half life 4hrs	305.3	20	20	20	20	20	20	20	20	20	20	20	20	20	20	
	152.6	8	8	8	8	8	8	8	8	8	8	8	8	8	8	
Etoposide PO <sup>2</sup>	600															
50 mg/m2	300	70		70		70		70		70		70		70		
days 1-21 of 28	150	44	33	44	33	44	33	44	33	44	33	44	33	44	33	
Half life 6.5hrs	75	20	20	x	20	20	x	20	20	x	20	20	x	20	20	x
	37.5	8	8	x	8	8	x	8	8	x	8	8	x	8	8	x
Romidepsin <sup>3</sup>	1000															
14 mg/m2	500															
IV days 1,8,15	250	x														
Half life 3hrs	125	x														
	62.5	x	x													
	31.3	x	x													
	15.7	x	x	x												
	7.6	x	x	x												
	3.8	70	61	60	60											
	1.9	50	50	46	40											
	1	65	24	22	18	65										
	0.5	50	16	13	13	50										
Etoposide PO	600															
50 mg/m2	300	70			21		x			x			x		x	
days 1-21 of 28	150	61	61		16	x		x	x		x	x		x	x	
Half life 6.5hrs	75	60	60	60		13	x	x		x	x	x		x	x	x
	37.5	60	60	60	60	12	x	x	x	x	x	x	x	x	x	x

1. Fiskus W., et al. (2012) J Clin Oncol  
 2. VePesid (etoposide) for injection and capsules [package insert] Bristol-Myers Squibb Co., Princeton, NJ; 2004. 3. Istodax<sup>®</sup> (romidepsin) for injection [package insert] Gloucester Pharmaceuticals, Inc., Cambridge, MA; 2009.

CI<0.6
CI=0.6-0.9
CI>0.9

**Fig 5. Clinical schedules and corresponding PK predicted activities for combinations of interest.** Dosing schedules for a 7-day treatment of oral etoposide paired with SP2509 and romidepsin. Plasma concentrations and estimated half-life for single-drug administration are derived from sources listed. Values in red indicate plasma concentrations comparable to experimental concentrations used. Values in boxes represent expected FA at given concentrations. Color represents amount of synergy expected. Gray boxes represent untested concentration combinations.

<https://doi.org/10.1371/journal.pone.0222228.g005>

interest in a malignancy like ES which is characterized by a translocation altering transcriptional control. HDACs are involved in a broad number of biological pathways, and interruption of their function can result in a plethora of transcriptional and functional consequences [41]. Sankar et. al. demonstrated that transcriptional repression of EWS-FLI1 is mediated through direct binding of the NuRD complex and that NuRD-associated HDAC and LSD1 functions are vital to this repression [3].

Of additional interest is the fact that we also saw synergistic activity when SP2509 was paired with romidepsin. These findings are consistent with other studies that investigated the co-administration of LSD1 and HDAC inhibitors in other cancer models as well as recent developments with a dual LSD-1/HDAC hybrid inhibitor [19, 42–44]. Although the most significant FA values we obtained with romidepsin were with drugs that utilized a different

mechanism of action, our findings of synergism with SP2509 suggest that the addition of both agents into the current ES treatment could prove beneficial, but further investigation is required.

The methods presented here demonstrate a comprehensive, reproducible, and high-throughput method for exploring antitumor effects of combinations of therapies at clinically achievable concentrations. In particular we discovered that combinations of SP2509 with currently utilized conventional chemotherapies demonstrate largely synergistic activity against ES cell lines. Several combinations seem to have translational promise. Combining SP2509 with oral etoposide would maximize the potential time that both agents can be maintained at therapeutic levels. Combining with VIT would be of interest as well and consideration for timing of SP2509 should be further considered. Additional explorations of these combinations through available murine models are recommended as well as extended assays to see the effects of long-term drug treatment.

## Supporting information

**S1 Fig. All order of addition results including two-drug, three-drug, and four-drug combinations as discussed in Fig 3. a) A673 (2250 cells), b) TC32 (4500 cells), c) A673 (4500 cells).** (TIF)

**S1 Table.** A) Average  $IC_{50} \pm$  standard error. B)  $IC_{50} \pm$  standard error as a % of  $C_{max}$ . C)  $IC_{50} \pm$  standard error with conditional formatting indicating %  $C_{max}$ . (TIFF)

**S2 Table. Full table of two-drug combinations.** (DOCX)

**S3 Table. Top combination treatment regimens based on a combination of FA and CI.** (TIF)

## Acknowledgments

We thank Dr. Kathleen Pishas for critical review of the manuscript.

## Author Contributions

**Conceptualization:** Darcy Welch, Elliot Kahen, Andrew S. Brohl, Christopher L. Cubitt, Damon R. Reed.

**Data curation:** Darcy Welch, Elliot Kahen, Brooke Fridley, Damon R. Reed.

**Formal analysis:** Darcy Welch, Elliot Kahen, Brooke Fridley.

**Funding acquisition:** Damon R. Reed.

**Investigation:** Darcy Welch, Elliot Kahen.

**Methodology:** Darcy Welch, Elliot Kahen, Brooke Fridley, Andrew S. Brohl, Christopher L. Cubitt, Damon R. Reed.

**Project administration:** Damon R. Reed.

**Resources:** Damon R. Reed.

**Supervision:** Damon R. Reed.

**Validation:** Elliot Kahen.

**Visualization:** Darcy Welch, Elliot Kahen, Brooke Fridley.

**Writing – original draft:** Darcy Welch.

**Writing – review & editing:** Darcy Welch, Elliot Kahen, Brooke Fridley, Andrew S. Brohl, Christopher L. Cubitt, Damon R. Reed.

## References

1. Gorlick R, Janeway K, Lessnick S, Randall RL, Marina N, Committee COGBT. Children's Oncology Group's 2013 blueprint for research: bone tumors. *Pediatr Blood Cancer*. 2013; 60(6):1009–15. <https://doi.org/10.1002/pbc.24429> PMID: 23255238; PubMed Central PMCID: PMC4610028.
2. Delattre O, Zucman J, Plougastel B, Desmaziere C, Melot T, Peter M, et al. Gene fusion with an ETS DNA-binding domain caused by chromosome translocation in human tumours. *Nature*. 1992; 359(6391):162–5. <https://doi.org/10.1038/359162a0> PMID: 1522903
3. Sankar S, Bell R, Stephens B, Zhuo R, Sharma S, Bearss DJ, et al. Mechanism and relevance of EWS/FLI-mediated transcriptional repression in Ewing sarcoma. *Oncogene*. 2013; 32(42):5089–100. <https://doi.org/10.1038/onc.2012.525> PMID: 23178492; PubMed Central PMCID: PMC3899696.
4. Brohl AS, Solomon DA, Chang W, Wang J, Song Y, Sindiri S, et al. The genomic landscape of the Ewing Sarcoma family of tumors reveals recurrent STAG2 mutation. *PLoS Genet*. 2014; 10(7): e1004475. <https://doi.org/10.1371/journal.pgen.1004475> PMID: 25010205; PubMed Central PMCID: PMC4091782.
5. Crompton BD, Stewart C, Taylor-Weiner A, Alexe G, Kurek KC, Calicchio ML, et al. The genomic landscape of pediatric Ewing sarcoma. *Cancer Discov*. 2014; 4(11):1326–41. <https://doi.org/10.1158/2159-8290.CD-13-1037> PMID: 25186949.
6. Tirode F, Surdez D, Ma X, Parker M, Le Deley MC, Bahrami A, et al. Genomic Landscape of Ewing Sarcoma Defines an Aggressive Subtype with Co-Association of STAG2 and TP53 Mutations. *Cancer Discovery*. 2014; 4(11):1342–53. <https://doi.org/10.1158/2159-8290.CD-14-0622> PMID: 25223734
7. Erkizan HV, Kong Y, Merchant M, Schlottmann S, Barber-Rotenberg JS, Yuan L, et al. A small molecule blocking oncogenic protein EWS-FLI1 interaction with RNA helicase A inhibits growth of Ewing's sarcoma. *Nat Med*. 2009; 15(7):750–6. <https://doi.org/10.1038/nm.1983> PMID: 19584866; PubMed Central PMCID: PMC2777681.
8. Wang Y, Zhang H, Chen Y, Sun Y, Yang F, Yu W, et al. LSD1 is a subunit of the NuRD complex and targets the metastasis programs in breast cancer. *Cell*. 2009; 138(4):660–72. Epub 2009/08/26. <https://doi.org/10.1016/j.cell.2009.05.050> PMID: 19703393.
9. Feng Z, Yao Y, Zhou C, Chen F, Wu F, Wei L, et al. Pharmacological inhibition of LSD1 for the treatment of MLL-rearranged leukemia. *J Hematol Oncol*. 2016; 9:24. Epub 2016/03/15. <https://doi.org/10.1186/s13045-016-0252-7> PMID: 26970896; PubMed Central PMCID: PMC4789278.
10. Alsaquer SF, Tashkandi MM, Kartha VK, Yang Y-T, Alkheriji Y, Salama A, et al. Inhibition of lsd1 epigenetically attenuates oral cancer growth and metastasis. *Oncotarget*. 2017; 8(43):73372–86. Epub 07/27/17. <https://doi.org/10.18632/oncotarget.19637> PubMed Central PMCID: PMC5650269. PMID: 29088714
11. Fang J, Landersdorfer CB, Cirincione B, Jusko WJ. Study reanalysis using a mechanism-based pharmacokinetic/pharmacodynamic model of pramlintide in subjects with type 1 diabetes. *AAPS J*. 2013; 15(1):15–29. <https://doi.org/10.1208/s12248-012-9409-7> PMID: 23054970; PubMed Central PMCID: PMC3535104.
12. Sankar S, Theisen ER, Bearss J, Mulvihill T, Hoffman LM, Sorna V, et al. Reversible LSD1 inhibition interferes with global EWS/ETS transcriptional activity and impedes Ewing sarcoma tumor growth. *Clin Cancer Res*. 2014; 20(17):4584–97. <https://doi.org/10.1158/1078-0432.CCR-14-0072> PMID: 24963049; PubMed Central PMCID: PMC4155010.
13. McGrath JP, Williamson KE, Balasubramanian S, Odate S, Arora S, Hatton C, et al. Pharmacological Inhibition of the Histone Lysine Demethylase KDM1A Suppresses the Growth of Multiple Acute Myeloid Leukemia Subtypes. *Cancer Res*. 2016; 76(7):1975–88. Epub 2016/02/04. <https://doi.org/10.1158/0008-5472.CAN-15-2333> PMID: 26837761.
14. Sehwat A, Gao L, Wang Y, Bankhead A, 3rd, McWeeney SK, King CJ, et al. LSD1 activates a lethal prostate cancer gene network independently of its demethylase function. *Proc Natl Acad Sci U S A*. 2018; 115(18):E4179–E88. Epub 2018/03/28. <https://doi.org/10.1073/pnas.1719168115> PMID: 29581250; PubMed Central PMCID: PMC5939079.

15. Mohammad HP, Smitheman KN, Kamat CD, Soong D, Federowicz KE, Van Aller GS, et al. A DNA Hypomethylation Signature Predicts Antitumor Activity of LSD1 Inhibitors in SCLC. *Cancer Cell*. 2015; 28(1):57–69. Epub 2015/07/16. <https://doi.org/10.1016/j.ccell.2015.06.002> PMID: 26175415.
16. Maes T, Mascaro C, Tirapu I, Estiarte A, Ciceri F, Lunardi S, et al. ORY-1001, a Potent and Selective Covalent KDM1A Inhibitor, for the Treatment of Acute Leukemia. *Cancer Cell*. 2018; 33(3):495–511 e12. Epub 2018/03/06. <https://doi.org/10.1016/j.ccell.2018.02.002> PMID: 29502954.
17. Romo-Morales A, Aladowicz E, Blagg J, Gatz SA, Shipley JM. Catalytic inhibition of KDM1A in Ewing sarcoma is insufficient as a therapeutic strategy. *Pediatr Blood Cancer*. 2019; 66(9):e27888. Epub 2019/06/18. <https://doi.org/10.1002/pbc.27888> PMID: 31207107.
18. Sonnemann J, Zimmerman M, Marx C, Ebert F, Becker S, Lauterjung M-L, et al. LSD1 (KDM1A)-independent effects of the LSD1 inhibitor SP2509 in cancer cells. *British Journal of Haematology*. 2018; 183:491–524. Epub 12/03/17. <https://doi.org/10.1111/bjh.14983> PubMed Central PMCID: PMC29205263 PMID: 29205263
19. Sonnemann J, Dreyer L, Hartwig M, Palani CD, Hong LTT, Klier U, et al. Histone deacetylase inhibitors induce cell death and enhance the apoptosis-inducing activity of TRAIL in Ewing's sarcoma cells. *Journal of Cancer Research and Clinical Oncology*. 2007; 133(11):847–58. <https://doi.org/10.1007/s00432-007-0227-8> PMID: 17486365
20. Shi YJ, Matson C, Lan F, Iwase S, Baba T, Shi Y. Regulation of LSD1 histone demethylase activity by its associated factors. *Mol Cell*. 2005; 19(6):857–64. Epub 2005/09/06. <https://doi.org/10.1016/j.molcel.2005.08.027> PMID: 16140033.
21. Thomas S, Aggarwal R, Jahan T, Ryan C, Troung T, Cripps AM, et al. A phase I trial of panobinostat and epirubicin in solid tumors with a dose expansion in patients with sarcoma. *Ann Oncol*. 2016; 27(5):947–52. Epub 2016/02/24. <https://doi.org/10.1093/annonc/mdw044> PMID: 26903311; PubMed Central PMCID: PMC4843187.
22. Cassier PA, Lefranc A, Amela EY, Chevreau C, Bui BN, Lecesne A, et al. A phase II trial of panobinostat in patients with advanced pretreated soft tissue sarcoma. A study from the French Sarcoma Group. *Br J Cancer*. 2013; 109(4):909–14. Epub 2013/08/08. <https://doi.org/10.1038/bjc.2013.442> PMID: 23922114; PubMed Central PMCID: PMC3749588.
23. Kahen E, Yu D, Harrison DJ, Clark J, Hingorani P, Cubitt CL, et al. Identification of clinically achievable combination therapies in childhood rhabdomyosarcoma. *Cancer Chemother Pharmacol*. 2016; 78(2):313–23. Epub 2016/06/22. <https://doi.org/10.1007/s00280-016-3077-8> PMID: 27324022; PubMed Central PMCID: PMC4965487.
24. Yu D, Kahen E, Cubitt CL, McGuire J, Kreaehling J, Lee J, et al. Identification of Synergistic, Clinically Achievable, Combination Therapies for Osteosarcoma. *Sci Rep*. 2015; 5:16991. Epub 2015/11/26. <https://doi.org/10.1038/srep16991> PMID: 26601688; PubMed Central PMCID: PMC4658502.
25. Goldsby RE, Fan TM, Villaluna D, Wagner LM, Isakoff MS, Meyer J, et al. Feasibility and dose discovery analysis of zoledronic acid with concurrent chemotherapy in the treatment of newly diagnosed metastatic osteosarcoma: a report from the Children's Oncology Group. *Eur J Cancer*. 2013; 49(10):2384–91. Epub 2013/05/15. <https://doi.org/10.1016/j.ejca.2013.03.018> PMID: 23664013; PubMed Central PMCID: PMC3689577.
26. Meyers PA, Schwartz CL, Krailo M, Kleinerman ES, Betcher D, Bernstein ML, et al. Osteosarcoma: a randomized, prospective trial of the addition of ifosfamide and/or muramyl tripeptide to cisplatin, doxorubicin, and high-dose methotrexate. *J Clin Oncol*. 2005; 23(9):2004–11. Epub 2005/03/19. <https://doi.org/10.1200/JCO.2005.06.031> PMID: 15774791.
27. Pishas KI, Drenberg CD, Taslim C, Theisen ER, Johnson KM, Saund RS, et al. Therapeutic Targeting of KDM1A/LSD1 in Ewing Sarcoma with SP-2509 Engages the Endoplasmic Reticulum Stress Response. *Molecular Cancer Therapeutics*. 2018; 17(9):1902–16. <https://doi.org/10.1158/1535-7163.MCT-18-0373> PMID: 29997151
28. El-Najjar N, Ketola RA, Nissila T, Mauriala T, Antopolsky M, Janis J, et al. Impact of protein binding on the analytical detectability and anticancer activity of thymoquinone. *J Chem Biol*. 2011; 4(3):97–107. Epub 2012/01/10. <https://doi.org/10.1007/s12154-010-0052-4> PMID: 22229047; PubMed Central PMCID: PMC3124627.
29. Chou T-C. Theoretical Basis, Experimental Design, and Computerized Simulation of Synergism and Antagonism in Drug Combination Studies. *Pharmacological Reviews*. 2006; 58(3):621–81. <https://doi.org/10.1124/pr.58.3.10> PMID: 16968952
30. Wagner LM. Fifteen years of irinotecan therapy for pediatric sarcoma: where to next? *Clin Sarcoma Res*. 2015; 5:20. Epub 2015/09/01. <https://doi.org/10.1186/s13569-015-0035-x> PMID: 26322224; PubMed Central PMCID: PMC4552408.



31. Palmerini E, Jones RL, Setola E, Picci P, Marchesi E, Luksch R, et al. Irinotecan and temozolomide in recurrent Ewing sarcoma: an analysis in 51 adult and pediatric patients. *Acta Oncol.* 2018; 57(7):958–64. Epub 2018/03/14. <https://doi.org/10.1080/0284186X.2018.1449250> PMID: 29533113.
32. Crompton BD, Stewart C, Taylor-Weiner A, Alexe G, Kurek KC, Calicchio ML, et al. The Genomic Landscape of Pediatric Ewing Sarcoma. *Cancer Discovery.* 2014; 4(11):1326–41. <https://doi.org/10.1158/2159-8290.CD-13-1037> PMID: 25186949
33. Womer RB, West DC, Krailo MD, Dickman PS, Pawel BR, Grier HE, et al. Randomized controlled trial of interval-compressed chemotherapy for the treatment of localized Ewing sarcoma: a report from the Children's Oncology Group. *J Clin Oncol.* 2012; 30(33):4148–54. <https://doi.org/10.1200/JCO.2011.41.5703> PMID: 23091096; PubMed Central PMCID: PMC3494838.
34. Reed DR, Hayashi M, Wagner L, Binitie O, Stepan DA, Brohl AS, et al. Treatment pathway of bone sarcoma in children, adolescents, and young adults. *Cancer.* 2017; 123(12):2206–18. <https://doi.org/10.1002/cncr.30589> PMID: 28323337; PubMed Central PMCID: PMC5485018.
35. Rudolph T, Yonezawa M, Lein S, Heidrich K, Kubicek S, Schafer C, et al. Heterochromatin formation in *Drosophila* is initiated through active removal of H3K4 methylation by the LSD1 homolog SU(VAR)3-3. *Mol Cell.* 2007; 26(1):103–15. Epub 2007/04/17. <https://doi.org/10.1016/j.molcel.2007.02.025> PMID: 17434130.
36. Hayami S, Kelly JD, Cho HS, Yoshimatsu M, Unoki M, Tsunoda T, et al. Overexpression of LSD1 contributes to human carcinogenesis through chromatin regulation in various cancers. *Int J Cancer.* 2011; 128(3):574–86. Epub 2010/03/25. <https://doi.org/10.1002/ijc.25349> PMID: 20333681.
37. Zöllner SK, Selvanathan SP, Graham GT, Commins RMT, Hong SH, Moseley E, et al. Inhibition of the oncogenic fusion protein EWS-FLI1 causes G2-M cell cycle arrest and enhanced vincristine sensitivity in Ewing's sarcoma. *Science Signaling.* 2017; 10(499). <https://doi.org/10.1126/scisignal.aam8429> PMID: 28974650
38. May WA, Grigoryan RS, Keshelava N, Cabral DJ, Christensen LL, Jenabi J, et al. Characterization and drug resistance patterns of Ewing's sarcoma family tumor cell lines. *PLoS One.* 2013; 8(12):e80060. <https://doi.org/10.1371/journal.pone.0080060> PMID: 24312454; PubMed Central PMCID: PMC3846563.
39. Franzetti GA, Laud-Duval K, van der Ent W, Brisac A, Irondelle M, Aubert S, et al. Cell-to-cell heterogeneity of EWSR1-FLI1 activity determines proliferation/migration choices in Ewing sarcoma cells. *Oncogene.* 2017; 36(25):3505–14. Epub 2017/01/31. <https://doi.org/10.1038/onc.2016.498> PMID: 28135250; PubMed Central PMCID: PMC5541267.
40. Gupta S, Weston A, Bearrs J, Thode T, Neiss A, Soldi R, et al. Reversible lysine-specific demethylase 1 antagonist HCI-2509 inhibits growth and decreases c-MYC in castration- and docetaxel-resistant prostate cancer cells. *Prostate Cancer Prostatic Dis.* 2016; 19(4):349–57. Epub 2016/06/29. <https://doi.org/10.1038/pcan.2016.21> PMID: 27349498; PubMed Central PMCID: PMC5133270 holder of Salaris Pharmaceuticals. SG's spouse is an equity holder of Salaris Pharmaceuticals. The remaining authors declare no conflicts of interest.
41. Sato T, Cesaroni M, Chung W, Panjarian S, Tran A, Madzo J, et al. Transcriptional Selectivity of Epigenetic Therapy in Cancer. *Cancer Research.* 2017; 77(2):470–81. <https://doi.org/10.1158/0008-5472.CAN-16-0834> PMID: 27879268
42. Haydn T, Metzger E, Schuele R, Fulda S. Concomitant epigenetic targeting of LSD1 and HDAC synergistically induces mitochondrial apoptosis in rhabdomyosarcoma cells. *Cell Death Dis.* 2017; 8(6):e2879. Epub 2017/06/16. <https://doi.org/10.1038/cddis.2017.239> PMID: 28617441; PubMed Central PMCID: PMC5520898.
43. Fiskus W, Sharma S, Shah B, Portier BP, Devaraj SG, Liu K, et al. Highly effective combination of LSD1 (KDM1A) antagonist and pan-histone deacetylase inhibitor against human AML cells. *Leukemia.* 2014; 28(11):2155–64. Epub 2014/04/05. <https://doi.org/10.1038/leu.2014.119> PMID: 24699304; PubMed Central PMCID: PMC4739780.
44. Kalin JH, Wu M, Gomez AV, Song Y, Das J, Hayward D, et al. Targeting the CoREST complex with dual histone deacetylase and demethylase inhibitors. *Nat Commun.* 2018; 9(1):53. Epub 2018/01/06. <https://doi.org/10.1038/s41467-017-02242-4> PMID: 29302039; PubMed Central PMCID: PMC5754352.